Technological University Dublin
ARROW@TU Dublin

Conference papers | School of Electrical and Electronic Engineering

2010-09-04

# The Application of Multi Frequency Resonant Controllers in in a DFIG to Improve Performance by Reducing Unwanted Power and Torque Pulsations and Reducing Current Harmonics.

Joseph Kearney
*Technological University Dublin*, joseph.kearney@tudublin.ie

Michael Conlon
*Technological University Dublin*, michael.conlon@tudublin.ie

Eugene Coyle
*Technological University Dublin*, Eugene.Coyle@tudublin.ie

Follow this and additional works at: https://arrow.tudublin.ie/engscheleart

 Part of the Electrical and Electronics Commons, and the Power and Energy Commons

## Recommended Citation

Kearney, Joseph; Conlon, Michael; and Coyle, Eugene, "The Application of Multi Frequency Resonant Controllers in in a DFIG to Improve Performance by Reducing Unwanted Power and Torque Pulsations and Reducing Current Harmonics." (2010). *Conference papers*. 224.
https://arrow.tudublin.ie/engscheleart/224

This Conference Paper is brought to you for free and open access by the School of Electrical and Electronic Engineering at ARROW@TU Dublin. It has been accepted for inclusion in Conference papers by an authorized administrator of ARROW@TU Dublin. For more information, please contact arrow.admin@tudublin.ie, aisling.coyne@tudublin.ie.

This work is licensed under a Creative Commons Attribution-Noncommercial-Share Alike 4.0 License

# The Application of Multi Frequency Resonant Controllers in in a DFIG to Improve Performance by Reducing Unwanted Power and Torque Pulsations and Reducing Current Harmonics.


Joseph Kearney
*Dublin Institute of Technology, Ireland*
Joseph.kearney@dit.ie

Michael F Conlon
*Dublin Institute of Technology, Ireland*
Michael.Conlon@dit.ie

Eugene Coyle
*Dublin Institute of Technology, Ireland*
Eugene.Coyle@dit.ie



***Abstract*- The paper describes a method to control the rotor-side and grid side converters in a DFIG when subjected to the effects of network voltage unbalance conditions. Multi Frequency Resonant Controllers are incorporated into the grid side and rotor side converters to assist in the control functions. The Resonant Controllers are tuned to twice the network frequency to assist in the control of power and torque pulsations and to three times the network frequency to assist in the control of the generated third harmonic currents. A DFIG model is implemented in Matlab/Simulink and simulations show the reduction in power and torque oscillations and a reduction in the 3rd harmonic currents generated as a result of the applied voltage unbalance.**



***Index Terms*—DFIG, Voltage Unbalance, Wind Energy**


## I. Introduction

In a DFIG both the stator and the rotor converter are connected directly to the grid and thus any voltage problems on the network can affect both the induction generator and the rotor converter. The process described in this paper involves modifying the standard DFIG control structures of both the rotor-side and the grid-side converters. The control structures combine proportional integral (PI) controller and parallel resonant (R) controllers in a multi-frequency proportional resonant (MFPR) controller implemented in the positive stator voltage orientated synchronous reference frame (SVO) [2, 3].

The resonant controllers are incorporated into the rotor side and grid side converters to assist in the control of the power, torque and dc link oscillations due to network voltage unbalance conditions and also to control 3rd harmonic currents generated. The method investigated in this paper also integrates the control variables of both the rotor-side and grid-side converters in a coordinated fashion and shows it is possible to reduce both the DFIG power and torque pulsations.

## II. Simulation Study

The DFIG wind turbine in this study is modelled in Matlab/Simulink [1] to analyse the behaviour of the DFIG to grid voltage unbalance. The system under investigation consists of a single DFIG connected to a simple network and further details can be obtained in [10].

## III. Method of Controlling DFIG during Voltage Unbalance Conditions

To reduce the power and torque pulsations as a result of network voltage unbalance it is necessary to modify the control structure of the rotor side converter. The traditional control structure of a DFIG can be modified to incorporate routines for positive and negative sequence control [3, 6, 8]. The idea is to control the positive and negative sequence components independently.

In an unbalanced network the stator apparent power can be expressed in terms of positive and negative sequence components [3, 4, 5]. Due to these components it is necessary to analyse the DFIG per-phase equivalent circuit in the positive and negative sequence dq reference frames.

During network voltage unbalance conditions and assuming no zero sequence components the positive and negative sequence currents of the fundamental frequency and the 3rd harmonic currents at the frequencies of $-2\omega_e$ and $3\omega_e$ are investigated in this paper.

The positive, negative and 3rd harmonic reference frames can be described by Fig. 1, where both the rotor side converter and grid side converter are controlled in the SVO, (stator voltage reference frame). Observing Fig. 1 the transformation between $\alpha\beta$, $dq^+$, $dq^-$ and $dq^{3+}$ reference frames is given as:

$$V_{dq}^{+} = V_{\alpha\beta} e^{-j\omega_e t}, \quad V_{dq}^{-} = V_{\alpha\beta} e^{j\omega_e t} \tag{1}$$

$$V_{dq}^{+} = V_{dq}^{-} e^{-2j\omega_e t}, \quad V_{dq}^{-} = V_{dq}^{+} e^{2j\omega_e t} \tag{2}$$

$$V_{dq}^{+} = V_{dq}^{3+} e^{2j\omega_e t}, \quad V_{dq}^{3+} = V_{dq}^{+} e^{-2j\omega_e t} \tag{3}$$

where superscripts (+) and (–) represent the positive and negative sequence reference frames, respectively.

Including the third harmonic components the voltage and current vectors can be expressed in terms of the positive and negative sequence and harmonic components as:

$$F_{dqs}^{+} = F_{dqs+}^{+} + F_{dqs-}^{-}.e^{-2j\omega_e t} + F_{dqs3+}^{3+}.e^{2j\omega_e t} \tag{4}$$

$F_{dqs}^{3+}{}_{3+}$ refers to the 3rd harmonic components in the positive synchronous reference frame rotating at an angular velocity of $3\omega_e$. The previously defined negative sequence 2nd harmonic components rotate at a speed of $-2\omega_e$ (angle $-2\theta_e$; difference between positive axis ($d^+$) and negative sequence axis ($d^-$)) and the third harmonic components rotate at a speed of $+2\omega_e$ (angle $2\theta_e$; difference between 3rd harmonic axis ($d^+$) and positive axis ($d^+$)).

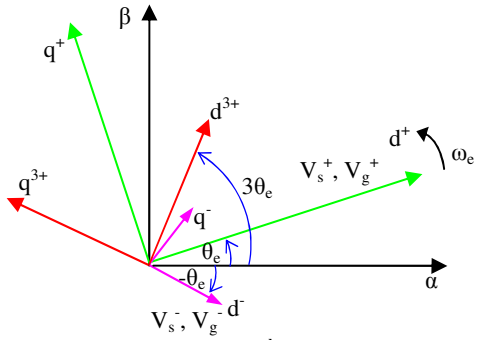


**Fig.. 1 dq Negative Sequence and 3rd Harmonic Rfeerence Frames**

## IV. ROTOR SIDE CONTROL

Using the equations for positive and negative sequence voltages and currents the apparent power of the converter can be calculated to improve the effects of voltage unbalance. The stator output apparent power can be described in the positive sequence reference frame as [3, 6]:

$$S = P_S + jQ_S = -\frac{3}{2}V_{dqs}^{+}I_{dqs}^{+*} \quad (5)$$

where the superscript (+) indicates the positive sequence reference frame and $V_{dq}^{+} = V_d^{+} + jV_q^{+}$ and $I_{dq}^{+} = I_d^{+} + jI_q^{+}$. Equation (5) can be expanded as [3, 4, 5, 8]:

$$S = -\frac{3}{2L_s}\begin{pmatrix}\left(V_{dqs+}^{+} + V_{dqs-}^{-}.e^{-j2\omega_e t}\right)\left(I_{dqs+}^{+*} + (I_{dqs-}^{-}.e^{-j2\omega_e t})^{*}\right)\\ -L_m\left(V_{dqs+}^{+} + V_{dqs-}^{-}.e^{-j2\omega_e t}\right)\left(I_{dqr+}^{+*} + (I_{dqr-}^{-}.e^{-j2\omega_e t})^{*}\right)\end{pmatrix} \quad (6)$$

When (6) is multiplied out and expanded in term of *d* and *q* positive and negative terms, the terms for active and reactive power can be obtained as:

$$S = P_s + jQ_s = \left(P_{so\_av} + P_{s\sin 2}\sin(2\omega_s t) + P_{s\cos 2}\cos(2\omega_s t)\right) + j\left(Q_{so\_av} + Q_{s\sin 2}\sin(2\omega_s t) + Q_{s\cos 2}\cos(2\omega_s t)\right) \quad (7)$$

where $P_{so,}$ $P_{s\ sin2,\ and}$ $P_{s\ cos2,}$ are the dc average, sine and cosine terms respectively, of twice the network frequency contained in the stator active power.

The sine and cosine terms in (7) can be equated to the expansion of (6) and then put equal to zero to obtain reference values for power and torque as illustrated in [6, 7, 8]. The negative sequence $I_{dqs}$ compensating reference values for the for power and torque are respectivelly:

$$I_{qr-}^{-} = \frac{2.V_{qs-}^{-}}{\omega_e L_m} + \frac{1}{V_{ds+}^{+}}\left(V_{ds-}^{-}I_{qr+}^{+} - V_{qs-}^{-}I_{dr+}^{+}\right) \quad (8)$$

$$I_{dr-}^{-} = -\frac{2.V_{ds-}^{-}}{\omega_e L_m} + \frac{1}{V_{ds+}^{+}}\left(V_{qs-}^{-}I_{qr+}^{+} - V_{ds-}^{-}I_{dr+}^{+}\right) \quad (9)$$

$$I_{dr-}^{-} = \frac{1}{V_{ds+}^{+}}\left[V_{qs-}^{-}.I_{dr+}^{+} - V_{ds-}^{-}.I_{qr+}^{+}\right] \quad (10)$$

$$I_{qr-}^{-} = \frac{1}{V_{ds+}^{+}}\left[V_{ds-}^{-}.I_{dr+}^{+} + V_{qs-}^{-}.I_{qr+}^{+}\right] \quad (11)$$

The decoupled compesating equations (8)-(11) are introduced into the stator voltage oriented control (SVO) of the rotor-side converter. These currents can be incorporated into the vector control scheme shown in Fig. 4 where *PI* controllers are applied to control rotor current and shaft speed.

## V. MULTI FREQUENCY PROPORTIONAL RESONANT CONTROLLER

Methods to control DFIG's during voltage unbalance conditions include parallel current control techniques operated in the positive and negative sequence reference frames to control the respective positive and negative sequence control currents $I_{dqr}^{+}{}_{+}$, $I_{dqr}^{-}{}_{-}$, $I_{dqg}^{+}{}_{+}$ and $I_{dqg}^{-}{}_{-}$ in the rotor side and grid side converters [7, 8]. An alternative method is to use a multi-frequency resonant controller in parallel with the *PI* current controller, called a multi-frequency proportional resonant (MFPR) controller [6]. The MFPR controller requires less positive and negative sequence decomposition and thus less time delay and errors [11].

According to (7) it is clear that during conditions of network voltage unbalance conditions the voltage, current and flux all contain both dc values of the positive sequence components and double frequency ($2\omega_e$) ac values of the negative sequence components in the $dq^{+}$ reference frame. The dc components are regulated normally by the *PI* controller however this controller cannot regulate the double frequency components. The negative sequence control currents $I_{dqr}^{-}{}_{-}$ have a frequency of $2\omega_e$ (100 Hz) and to control these currents adequately it is thus necessary to use a controller that is tuned to 100 Hz. Voltage unbalance can also introduce harmonic currents into power converters. In this paper the 3rd harmonic currents were found to be the most significant. The 3rd harmonic currents have a frequency of $3\omega_e$ (150 Hz) and to control these currents adequately it is thus necessary to use a controller that is tuned to 150 Hz. A multi-frequency proportional resonant (MFPR) controller is implemented in the rotor side current controller for directly controlling both the positive and negative sequence components [11, 12]. The voltage reference output of the MFPR controller can be described as:

$$V_{dqr}^{e+-} = \left((I_{dqr}^{e+*} + I_{dqr}^{e2+*} + I_{dqr}^{e3+*}) - I_{dqr}^{e+}\right)\begin{Bmatrix}k_p + \frac{k_i}{s} + k_{iR}\left(\frac{s}{s^2 + s2\omega_c + (2\omega_e)^2}\right)\\ +k_{iR}\left(\frac{s}{s^2 + s2\omega_c + (3\omega_e)^2}\right)\end{Bmatrix} \quad (14)$$

In (14) $\omega_e$ is the resonance frequency of the controller, $K_p$ and $K_i$ are the proportional gain and the integral gains respectively of the rotor side current controler. The reference currents $I_{dqr}^{e+*}$, $I_{dqr}^{e2+*}$, $I_{dqr}^{e3+*}$ are the positive sequence current, the negative sequence reference current and the third-harmonc reference current respectivelly, all transferred into the positive sequence reference frame.

The MFPR controller has a very high gain around the resonance frequency and it eliminates the steady state error between the reference and the measured signal. The width of the frequency band around the resonance point depends

on the integral gain value. A small value produces a very narrow band, whereas a large value produces a wider band. The cut-of frequency $\omega_c$ in (14) also increases the band-width. The Bode plots of the resonant controller for the negative sequence control ($2\omega_e$) and for 3rd harmonic control ($3\omega_e$) and for for integral gains $k_{iR}$ of 100, 200, 500, 1000 and 2000, with $\omega_c$ set to 5 are shown in Fig. 2.. As can be observed this type of controller can achieve a very high gain in a frequency band around the resonance frequency

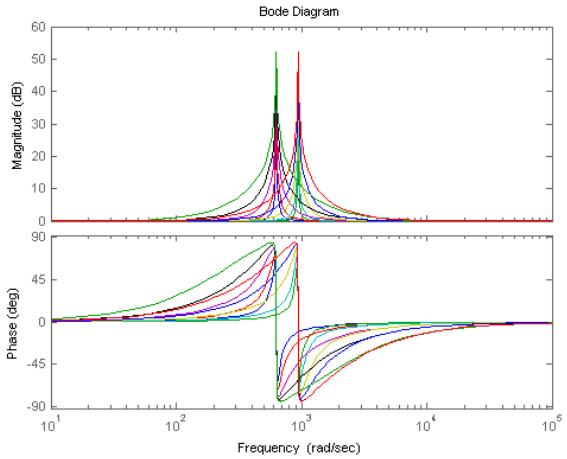


Figure 2: Bode plot of Resonant Controllers tuned to $2w_e$ and $3w_e$: gains ranging form 100 (narrow band) to 2000 (wide band).

A control scheme incorporating a *PI* controller in parallel with a resonant (*R*) controllers tuned to twice the network frequency (100 Hz) and three times the network fequency (150Hz) is implemented as shown in Fig. 4. The discrete *PI&R* controller shown is implemented in the $dq^+$ reference frame in the program Matlab/Simulink.

The resonant controllers for the 2nd and 3rd harmonic currents in the rotor side converter are given in the continuous and digital domans respectivelly as:

$$R_2 = \frac{sk_{ir}}{s^2 + 2s\omega_c + (2.2\pi.50)^2} = \frac{z.0.4993810^{-4} + 0 + 0.4993810^{-4}}{z^2 - z.1.99555 + 0.9995} \quad (15)$$

$$R_3 = \frac{sk_{ir}}{s^2 + 2s\omega_c + (3.2\pi.50)^2} = \frac{z.0.498910^{-4} + 0 + 0.498910^{-4}}{z^2 - z.1.99113703 + 1} \quad (16)$$

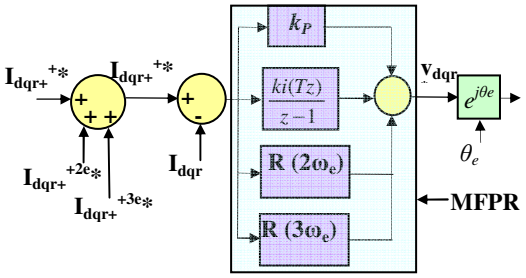


**Fig.. 3 Grid & Rotor Side MFPR Controllers**

The rotor currents are transformed into the positive sequence $dq^+$ and negative $dq^-$ sequence reference frames, using the rotor slip angle $\theta_{sl}$. Band-stop (notch) filters tuned at $2\omega_e$ are then used to remove the oscillating terms, and leave the respective positive and negative sequence control currents $I_{dqr}^{+}{}_{+}$ and $I_{dqr}^{-}{}_{-}$.

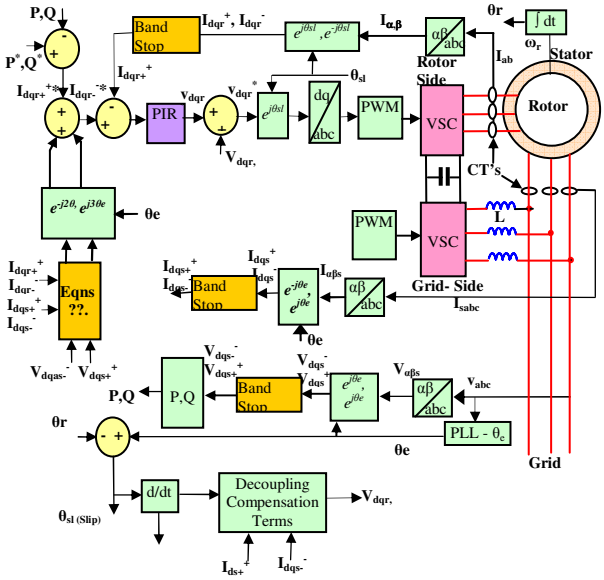


**Fig. 4. Rotor Side Converter Parallel Unbalance Control Structure**

The four reference currents $I_{dr}^{+*}{}_{+}$, $I_{qr}^{+*}{}_{+}$, $I_{dr}^{-*}{}_{-}$, $I_{qr}^{3+*}{}_{+}$ and $I_{dr}^{3+*}{}_{+}$ are all dc signals separated in the respective positive, negative and 3rd harmonic sequence reference frames as shown in Fig. 1. The negative sequence components obtained are then incorporated into the positive sequence control loop. In this paper reactive power control is not used and the reference $I_{qr}^{+}{}_{+}$ is set = 0.

## VI. GRID SIDE CONVERTER CONTROL

The control structure for the grid-side converter is based on the decoupled *d-q* vector control methods as previously outlined for the rotor-side converter and [12]. The grid-side converter controls the dc link voltage and can also control reactive power. Using the equations for positive and negative sequence voltages and currents the apparent power of the converter can be power can be described as [7]:

$$S = P_g + jQ_g = \frac{3}{2} V_{dqg}^{+} I_{dqg}^{+*} \quad (17)$$

And from [12]:

$$S = \frac{3}{2}.\left( \begin{array}{l} \left(V_{dqg+}^{+} + V_{dqg-}^{-}.e^{-j2\omega_e t} + V_{dqg3+}^{+3}.e^{j2\omega_e t}\right)x \\ \left(I_{dqg+}^{+*} + (I_{dqg-}^{-}.e^{-j2\omega_e t})^{*} + (I_{dqg3+}^{+3}.e^{j2\omega_e t})^{*}\right) \end{array} \right) \quad (18)$$

The positive, negative and 3rd harmonic sequence reference currents $I_{dg}^{+}{}_{+}$, $I_{qg}^{+}{}_{+}$, $I_{dg}^{-}{}_{-}$, $I_{qr}^{-}{}_{-}$, $I_{dg}^{3+}{}_{+}$ and $I_{qg}^{3+}{}_{+}$ are obtained as [12]:

$$I_{dg+}^{+} = \frac{1}{v_{dg+}^{+}} \left[ \begin{array}{l} \frac{2}{3} P_o - V_{dg-}^{-} I_{dg-}^{-} - V_{qg-}^{-} Ii_{qg-}^{-} \\ + V_{dg3+}^{3+} I_{dg3+}^{3+} + V_{dg3+}^{3+} I_{dg3+}^{3+} \end{array} \right] \quad (19)$$

$$I_{dg-}^{-} = \frac{1}{v_{dg+}^{+}} \left[ v_{dg-}^{-}.I_{dg+}^{+} + v_{qg-}^{-}.Ii_{qg+}^{+} \right] \quad (20)$$

$$I_{qg-}^{-} = \frac{1}{v_{dg+}^{+}}\left[v_{dg-}^{-}.i_{dg+}^{+} - v_{dg-}^{-}.i_{qg+}^{+}\right] \quad (21)$$

$$I_{dg+}^{3+} = -\frac{1}{v_{dg+}^{+}}\begin{bmatrix} V_{dg+}^{+}I_{dg-}^{-} + \left(V_{dg-}^{-} + V_{dg3+}^{3+}\right)I_{dg+}^{+} \\ + \left(V_{qg-}^{-} + V_{qg3+}^{3+}\right)I_{qg+}^{+} \end{bmatrix} \quad (22)$$

$$I_{qg+}^{3+} = -\frac{1}{v_{dg+}^{+}}\begin{bmatrix} V_{dg+}^{+}I_{qg-}^{-} + \left(V_{qg-}^{-} - V_{qg3+}^{3+}\right)I_{dg+}^{+} \\ - \left(V_{dg-}^{-} - V_{dg3+}^{3+}\right)I_{qg+}^{+} \end{bmatrix} \quad (23)$$

Similar to the rotor side converter a multi-frequency proportional resonant (MFPR) grid side current controller can be implemented for directly controlling both the positive and negative sequence components [11, 12]. The voltage reference output of the *PI&R* controller can be described as:

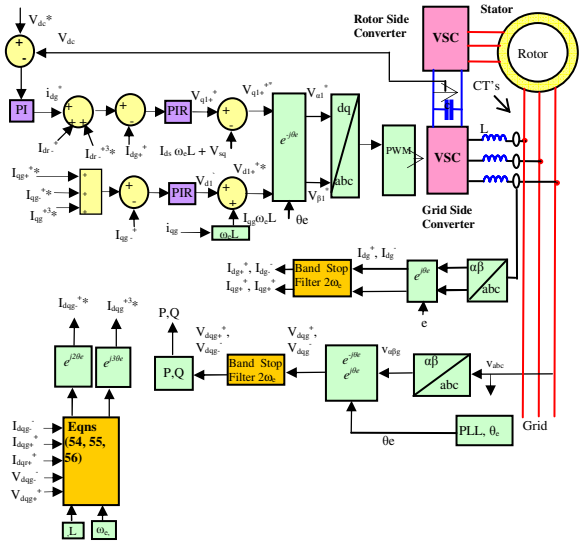


**Fig. 5. Grid Side Converter Control**

$$V_{dqg}^{e+`} = \left((I_{dqg}^{e+*} + I_{dqg}^{e2+*} + I_{dqg}^{e3+*}) - I_{dqg}^{e+}\right)\left\{\begin{aligned} &k_p + \frac{k_i}{s} + k_{iR}\left(\frac{s}{s^2 + s2\omega_c + (2\omega_c)^2}\right) \\ &+ k_{iR}\left(\frac{s}{s^2 + s2\omega_c + (3\omega_c)^2}\right) \end{aligned}\right\} \quad (24)$$

The control for the grid side converter is illustrated in Fig. 5.

## VII. Coordinated Control

A method to control both the power oscillations and the torque pulsations in a DFIG, by analysing the rotor side converter which controls the stator power in the stator flux oriented reference frame and the control of the grid side converter in the grid voltage reference frame was investigated in [9]. The total apparent power of a DFIG is [5]:

$$S = P_T + jQ_T = -\frac{3}{2}\left(V_{dqs}^{+}I_{dqs}^{*} + V_{dqr}^{+}I_{dqr}^{*}\right) \quad (25)$$

The total real power in equation (18) is the sum of the real power from the stator $P_s$ and the grid side converter $P_G$, $P_T = P_s + P_g$. Under voltage unbalance conditions the total real power can be described as [12]:

$$\begin{aligned} P_T = &\left(P_{s\_av} + P_{s\_\sin 2}\sin(2\theta_e) + P_{s\_\cos 2}\cos(2\theta_e)\right) \\ &+ \left(P_{og} + P_{s2g}\sin(2\theta_g) + P_{c2g}\cos(2\theta_g)\right) \end{aligned} \quad (26)$$

The rotor side converter and the grid side converter are both controlled in the grid or stator voltage reference frame (SVO), see Fig. 1 and therefore $\theta_e = \theta_g$ and (19) can be described as:

$$\begin{aligned} P_T = &(P_{s\_av} + P_{og}) + (P_{s\_\sin 2} + P_{s2g})\sin(2\theta_e) \\ &+ (P_{s\_\cos 2} + P_{c2g})\cos(2\theta_e t) \end{aligned} \quad (27)$$

In (27) letting $P_{s\_sin2} = -P_{s2g}$ and $P_{c\_cos2} = -P_{c2g}$ then the total real power becomes $P_T = (P_{s\_av} + P_{og})$. For $P_{s2g} = -P_{s\_sin2}$, and with the rotor side converter *d*-axis aligned with stator or grid voltage and the grid side converter *d*-axis also aligned with the grid voltage will result in $V_{qs}^{+}{}_{+} = V_{qg}^{+}{}_{+} = 0$ and (27) becomes [12]:

$$\begin{aligned} P_{s2g} = &\frac{3}{2}\left(V_{qg-}^{-}I_{dg+}^{+} - V_{dg-}^{-}I_{qg+}^{+} - 0 + V_{dg+}^{+}I_{qg-}^{-}\right) = \\ &\left\{ -P_{s\_\sin 2} = \frac{3}{2\omega_e L_s}\left(V_{qs-}^{-}V_{ds+}^{+} + 0 + 0 + V_{ds+}^{+}V_{qs-}^{-}\right)\right. \\ &\left. -\frac{3L_m}{2L_s}\left(V_{qs-}^{-}I_{dr+}^{+} - V_{ds-}^{-}I_{qr+}^{+} + 0 + V_{ds+}^{+}I_{qr-}^{-}\right)\right\} \end{aligned} \quad (28)$$

And solving (28) to get the grid side reference current $I_{qg}^{-}$:

$$\begin{aligned} I_{qg-}^{-} = &\frac{1}{V_{dg+}^{+}}\left[-V_{qg-}^{-}I_{dg+}^{+} + V_{dg-}^{-}I_{qg+}^{+}\right] + \frac{2}{\omega_e L_s V_{dg+}^{+}}\left(V_{qs-}^{-}V_{ds+}^{+}\right) \\ &-\frac{L_m}{L_s V_{dg+}^{+}}\left(V_{qs-}^{-}I_{dr+}^{+} - V_{ds-}^{-}I_{qr+}^{+} + V_{ds+}^{+}I_{qr-}^{-}\right) \end{aligned} \quad (29)$$

Similarly for $P_{s\_cos2} = -P_{c2g}$ the reference current $I_{dg-}$ can be obtained as:

$$\begin{aligned} I_{dg-}^{-} = &-\frac{1}{V_{dg+}^{+}}\left[V_{qg-}^{-}.I_{dg+}^{+} + V_{dg-}^{-}.I_{qg+}^{+}\right] + \frac{2}{V_{dg+}^{+}\omega_e L_s}\left(V_{ds+}^{+}V_{ds-}^{-}\right) \\ &-\frac{L_m}{V_{dg+}^{+}L_s}\left(V_{ds-}^{-}I_{dr+}^{+} + V_{qs-}^{-}I_{qr+}^{+} + V_{ds+}^{+}I_{dr-}^{-}\right) \end{aligned} \quad (30)$$

## VIII. Simulation Results

The control schemes of the rotor side and grid side converters as illustrated in Fig.4 and Fig. 5 were implemented in a model in the software program Matlab/Simulink. In the Simulink model a large single phase load is introduced at 0.5s resulting in a voltage unbalance of 8% appearing at the DFIG terminals. This level of voltage unbalance leads to the DFIG generating a current unbalance of 15%. The rise in the levels of voltage and current unbalance at 0.5s from the simulation are shown in Fig. 6.

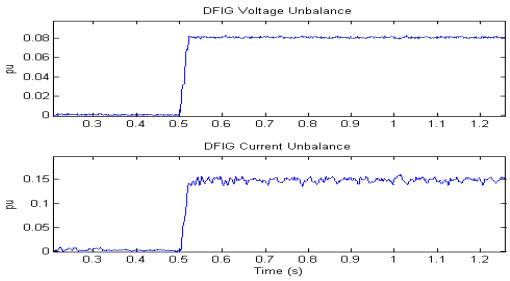


**Fig. 6. DFIG Voltage & Current Unbalance**

In the Matlab/Simulink model compensation techniques are applied at 0.6s. Fig. 6 shows plots of the torque, stator power, grid side power, the DFIG total power and the grid side and DFIG total harmonc currents. Fig. 7(a) illustrates the effects on the DFIG when voltage unbalance is introduced at 0.5s. It is clear that Torque pulsations and power oscillations occur at the stator and grid side of the DFIG. Also observed is the introduction of third-harmonic currents at the grid side and DFIG terminals. When Negative sequence voltage unbalance compensation is introduced in the rotor side and grid side converters at 0.6s the effects can be observed in Fig. 7(b).

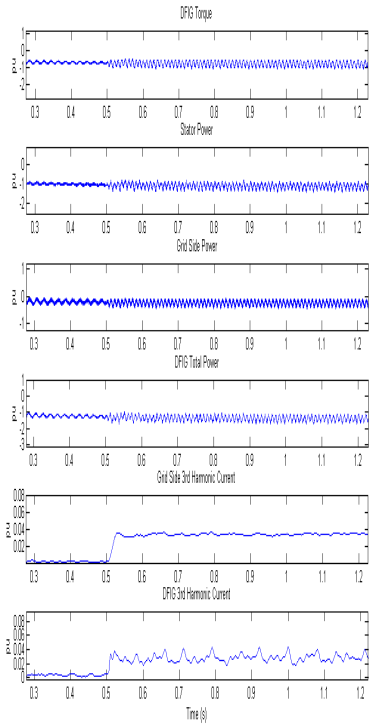


**Fig.. 7(a) DFIG Torque, Stator, Gird Side & Total Power and Grid Side & DFIG 3rd Harmonic Current**

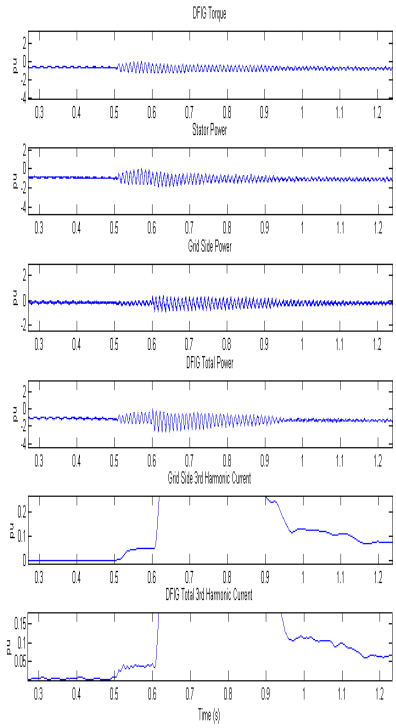


**Fig.. 7(b) DFIG Torque, Stator, Gird Side & Total Power and Grid Side & DFIG 3rd Harmonic Current**

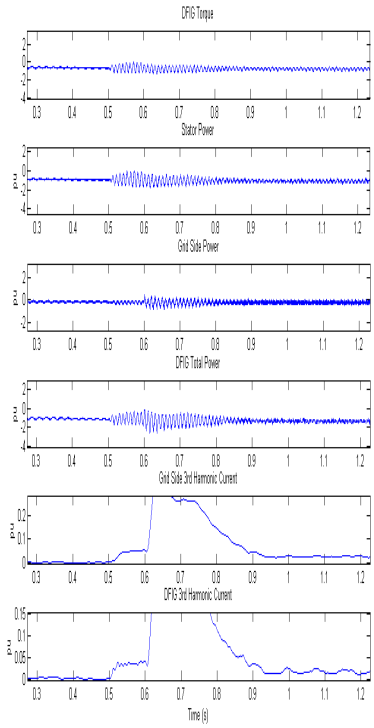


**Fig.. 7(c) DFIG Torque, Stator, Gird Side & Total Power and Grid Side & DFIG 3rd Harmonic Current**

The compensation technique using the MFPR is configured to control the torque pulsations and the total power oscillations. It can be obsevered that there is good reduction in the torque poulsations and the DFIG total power oscilation. The stator power oscillations are also reduced, however the grid side power oscilaltions are not substantially reduced. This is due to the grid side converter configured to control the DFIG total power oscillations. Also observed in Fig. 7(b) is the increase in third harmonic currents. Fig. 7(c) shows plots to the response of the DFIG when it is also controlled to reduce the amplitude of the 3rd harmonic currents. Where the control response of the torque, stator, grid and total powers are broadly similar to Fig. 7(b) it is clear that there is a reduction in the grid side 3rd harmonic currents and the DFIG total 3rd harmonic currents.

## IX. Conclusion

The control structures of the rotor side and grid side converters in a DFIG were modified to improve the performance during network voltage unbalance conditions. In particular modifications to the control structures to decrease the power and torque oscillation and 3rd harmonic currents was investigated. A model of a DFIG was implemented in Matlab/Simulink with a multi-frequency proportional resonant (MFPR) controller incorporated in the rotor side and grid side converters and

simulation results demonstrate the reduction in torque and power oscillations and 3rd harmonic currents.

## REFERENCES


1. Matlab. The Mathworks Inc.
2. M.F. Conlon and J. Kearney, "Negative Sequence Analysis of Induction Machines" 40th Universities Power Engineering Conference (UPEC), Cork, Ireland, 6th - 9th September 2005
3. Lie Xu, Yi Wang, "Dynamic Modelling and Control of DFIG-Based Turbines Under Unbalanced Network Conditions", *IEEE Transactions on Power Systems,* 2007. pp 314-323.
4. Yi Wang, Lie Xu, "Control of DFIG-Based Wind Generation Systems under Unbalanced Network Supply", *IEEE International, Electrical Machines and Drives Conference*, 2007, IEMDC 3-5th May '07. pp 430-435.
5. Jeong-Ik Jang, Young-Sin Kim, "Active and Reactive Power Control of DFIG for Wind Energy Conversion under Unbalanced Grid Voltage", *IEEE IPEMC Conference* 2006.
6. Hu Jia-bing, He Yi-kang, "Enhanced control of DFIG-using back-to-back PWM VSC under unbalanced grid voltage conditions", *Journal of Zhejiang University SCIENCE A,* China, 2007. pp 1330-1339.
7. Hong-Seok Song, Kwanghee Nam, "Dual Current Control for PWM Converter Under Unbalanced Input Voltage Conditions", *IEEE Transactions on Industrial Electronics*, vol. 46 no. 5, October 1999, pp 953-959.
8. J Kearney, M. F. Conlon, "Control Double-Fed Induction Generator Wind Turbine During Network Voltage Unbalance Conditions", *42nd Universities Power Engineering Conference (UPEC)*, Padua, Italy, 2nd - 5th September 2008.
9. Lie XU, "Coordinated Control of DFIG's Rotor and Grid Side Converters During Network Unbalance", *IEEE Transactions on Power Electronics,* vol. 23, no. 3, May 2008.
10. Joe Kearney, M. F. Conlon & E Coyle, "The Integrated Control of the Rotor Side and Grid Converters in a DFIG to Reduce Both Power and Torque Pulsations During Network Voltage Unbalance Conditions", in Proc. *43nd Universities Power Engineering Conference (UPEC),* Glasgow, Scotland, 1nd - 4th September 2009.
11. Jia-bing Hu, Yi-kang He, "Modelling and enhanced control of DFIG under unbalanced grid voltage conditions", Electrical Power Systems Research 79, 2009, pp 273-281.
12. Joe Kearney, M F Conlon & E Coyle, "The Control of Rotor Side and Grid Side Converters in a DFIG During Network Voltage Unbalance Conditions Using Resonant Current Controllers", EVRE Conference, Monaco, 24th- 28th March 2010, EVER10-288.